Journal of Chromatography, 545 (1991) 135–147
Elsevier Science Publishers B.V., Amsterdam

CHROM. 23 205

Generalized treatment of spatial and temporal column parameters, applicable to gas, liquid and supercritical fluid chromatography

II. Application to supercritical CO_2

D. E. MARTIRE* and R. L. RIESTER
Department of Chemistry, Georgetown University, Washington, DC 20057 (USA)
T. J. BRUNO
Thermophysics Division, National Institute of Standards and Technology, Boulder, CO 80303 (USA)
and
A. HUSSAM[a] and D. P. POE[b]
Department of Chemistry, Georgetown University, Washington, DC 20057 (USA)
(First received October 31st, 1990; revised manuscript received February 5th, 1991)

ABSTRACT

Equations derived in Part I [D. E. Martire, *J. Chromatogr.*, 461 (1989) 165] are used to calculate distribution functions, average densities and column profiles for supercritical fluid chromatography with carbon dioxide as the mobile phase. An approximation for the column-average capacity factor in terms of the local capacity factor is evaluated and conditions are given for its applicability.

INTRODUCTION

General equations have been derived for the spatial and temporal density distribution functions, average densities and column profiles of the mobile-phase fluid, and for the observed (apparent) capacity factors and column profiles of the solute components [1]. These equations are valid for all conditions where Darcy's law is valid, *i.e.*, as long as the flow is laminar and not turbulent. It has been shown in Part I [1] that the application of these equations is straightforward in the cases of gas and liquid chromatography. In capillary supercritical fluid chromatography (SFC), pressure drops over the length of the column are usually so small that the average density is close to the inlet density. Thus, the most interesting application is in packed-column SFC

[a] Present address: Department of Chemistry, George Mason University, Fairfax, VA 22030, USA.
[b] Present address: Department of Chemistry, University of Minnesota, Duluth, MN 55812, USA.

0021-9673/91/$03.50

because of the large pressure drops involved and the non-ideality and compressibility of the mobile phase.

In the present study, the equations are applied to SFC with carbon dioxide as the mobile phase. In order to apply these equations, reliable density, isothermal compressibility and viscosity data for the mobile phase are needed. A modified Benedict–Webb–Rubin (BWR) equation of state [2] was used to generate densities and isothermal compressibilities; available viscosity data were used to fit a polynomial expression for viscosity in terms of density and temperature. For a given inlet pressure, the outlet pressure will depend on several variables: the column length, type and porosity of packing, type of back-pressure regulator or restrictor used, etc. In this study, various inlet and outlet pressures were assumed and distribution functions, density averages and column profiles for the mobile phase were calculated. In order to generate average capacity factors and column profiles for the solutes, an expression for the local capacity factor was assumed.

The following equations from ref. 1 (written here in reduced form) are used in this study:

The spatial distribution function $D_x(\rho_R)$

$$D_x(\rho_R) = \eta_R^{-1}\rho_R(\partial P_R/\partial\rho_R)_T \tag{1}$$

The temporal distribution function $D_t(\rho_R)$

$$D_t(\rho_R) = \eta_R^{-1}\rho_R^2(\partial P_R/\partial\rho_R)_T \tag{2}$$

The spatial average mobile phase density $<\rho_R>_x$

$$<\rho_R>_x = \int_{\rho_{R,0}}^{\rho_{R,i}} \rho_R D_x(\rho_R)\mathrm{d}\rho_R / \int_{\rho_{R,0}}^{\rho_{R,i}} D_x(\rho_R)\mathrm{d}\rho_R \tag{3}$$

The temporal average mobile phase density, $<\rho_R>_t$

$$<\rho_R>_t = \int_{\rho_{R,0}}^{\rho_{R,i}} \rho_R D_t(\rho_R)\mathrm{d}\rho_R / \int_{\rho_{R,0}}^{\rho_{R,i}} D_t(\rho_R)\mathrm{d}\rho_R \tag{4}$$

The observed capacity factor, $<k'>_t$

$$<k'>_t = \int_{\rho_{R,0}}^{\rho_{R,i}} k' D_t(\rho_R)\mathrm{d}\rho_R / \int_{\rho_{R,0}}^{\rho_{R,i}} D_t(\rho_R)\mathrm{d}\rho_R \tag{5}$$

The fractional distance, x/L, when the local mobile phase density is ρ_R

$$x/L = \int_{\rho_R}^{\rho_{R,i}} D_x(\rho_R)\mathrm{d}\rho_R / \int_{\rho_{R,0}}^{\rho_{R,i}} D_x(\rho_R)\mathrm{d}\rho_R \tag{6}$$

The fractional time, τ_u/t_u, an unretained solute has spent on the column when the local density is ρ_R

$$\tau_u/t_u = \int_{\rho_R}^{\rho_{R,i}} D_t(\rho_R)d\rho_R / \int_{\rho_{R,o}}^{\rho_{R,i}} D_t(\rho_R)d\rho_R \tag{7}$$

The fractional solute migration time, τ_s/t_s, at ρ_R

$$\tau_s/t_s = \int_{\rho_R}^{\rho_{R,i}} (1 + k')D_t(\rho_R)d\rho_R / \int_{\rho_{R,o}}^{\rho_{R,i}} (1 + k')D_t(\rho_R)d\rho_R \tag{8}$$

In these equations the density (ρ), pressure (P) and viscosity (η) are normalized to reduced variables: $\rho_R = \rho/\rho_{cr}$, $P_R = P/P_{cr}$, $\eta_R = \eta/\eta^o$ where $\rho_{cr} = 0.468$ g/cm^3, $T_{cr} = 304.2$ K, $P_{cr} = 73.84$ bar and η^o is chosen as the viscosity at one bar for a given temperature. L refers to the column length measured from the inlet, t_u the holdup time of an unretained solute, t_s the solute retention time, k' the local capacity factor; the subscripts i and o refer to inlet and outlet conditions, respectively. The quantity $\eta_R^{-1}(\partial P_R/\partial \rho_R)_T$ which appears in both distribution functions will be referred to as the "core" of the distribution function.

The observed or apparent capacity factor is related to the local capacity factor and conditions are given for an approximation for the observed capacity factor in terms of the temporal average density. In addition, the separation factor, α, for two solutes a and b is calculated from

$$\alpha = \frac{<k'>_{t,b}}{<k'>_{t,a}} \tag{9}$$

THE EQUATION OF STATE

The Jacobsen–Stewart modification [2,3] of the BWR equation of state was used to generate reliable density (ρ) and isotherm derivative, $(\partial P_R/\partial \rho_R)_T$, predictions:

$$P = \rho RT + \sum_{i=1}^{32} N_i X_i \tag{10}$$

$$(\partial P/\partial \rho)_T = RT + \sum_{i=1}^{32} N_i X_i' \tag{11}$$

where $X_i' = (\partial X_i/\partial \rho)_T$.

The N_i coefficients for CO_2 were obtained from ref. 3 and are reproduced in column 2 of Table I. Expressions for the X_i and X_i' are given in columns 3 and 4 of Table I. ρ is the density in mol/l; P the pressure in bar, T the temperature in Kelvin; R = 0.083144 bar · l/mol · K. The equations are applicable for a temperature range from 215 to 1100 K and from 0 to 3000 bar with an overall accuracy of 0.3% in density [3]. Since the equation is explicit in pressure, density predictions were obtained using the bisection method [4].

TABLE I

COEFFICIENTS AND EXPRESSIONS OF EXTENDED BWR EQUATION FOR CO_2[a]

$F = \exp(-G\rho^2)$; $G = 0.88999644 \cdot 10^{-2}$; $F' = -2.0F\rho G$; $F21 = 3.0F\rho^2 + F'\rho^3$; $F22 = 5.0F\rho^4 + F'\rho^5$; $F23 = 7.0F\rho^6 + F'\rho^7$; $F24 = 9.0F\rho^8 + F'\rho^9$; $F25 = 11.0F\rho^{10} + F'\rho^{11}$; $F26 = 13.0F\rho^{12} + F'\rho^{13}$.

i	N	X	X'
1	$-0.9818510658 \cdot 10^{-2}$	ρ^2T	$2.0\rho T$
2	0.9950622673	$\rho^2T^{1/2}$	$2.0\rho T^{1/2}$
3	$-0.2283801603 \cdot 10^{2}$	ρ^2	2.0ρ
4	$0.2818276345 \cdot 10^{4}$	ρ^2/T	$2.0\rho/T$
5	$-0.3470012627 \cdot 10^{6}$	ρ^2/T^2	$2.0\rho/T^2$
6	$0.3947067091 \cdot 10^{-3}$	ρ^3T	$3.0\rho^2T$
7	-0.3255500001	ρ^3	$3.0\rho^2$
8	4.843200831	ρ^3/T	$3.0\rho^2/T$
9	$-0.3521815430 \cdot 10^{6}$	ρ^3/T^2	$3.0\rho^2/T^2$
10	$-0.3240536033 \cdot 10^{-4}$	ρ^4T	$4.0\rho^3T$
11	$0.4685966847 \cdot 10^{-1}$	ρ^4	$4.0\rho^3$
12	-7.545470121	ρ^4/T	$4.0\rho^3/T$
13	$-0.381894354 \cdot 10^{-4}$	ρ^5	$5.0\rho^4$
14	$-0.4421929339 \cdot 10^{-1}$	ρ^6/T	$6.0\rho^5/T$
15	$0.5169251681 \cdot 10^{2}$	ρ^6/T^2	$6.0\rho^5/T^2$
16	$0.2124509852 \cdot 10^{-2}$	ρ^7/T	$7.0\rho^6/T$
17	$-0.2610094748 \cdot 10^{-4}$	ρ^8/T	$8.0\rho^7/T$
18	$-0.888533389 \cdot 10^{-1}$	ρ^8/T^2	$8.0\rho^7/T^2$
19	$0.1552261794 \cdot 10^{-2}$	ρ^9/T^2	$9.0\rho^8/T^2$
20	$0.4150910049 \cdot 10^{6}$	ρ^3F/T^2	$F21/T^2$
21	$-0.1101739675 \cdot 10^{8}$	ρ^3F/T^3	$F21/T^3$
22	$0.2919905833 \cdot 10^{4}$	ρ^5F/T^2	$F22/T^2$
23	$0.1432546065 \cdot 10^{8}$	ρ^5F/T^4	$F22/T^4$
24	$0.1085742075 \cdot 10^{2}$	ρ^7F/T^2	$F23/T^2$
25	$-0.247799657 \cdot 10^{3}$	ρ^7F/T^3	$F23/T^3$
26	$0.1992935908 \cdot 10^{-1}$	ρ^9F/T^2	$F24/T^2$
27	$0.1027499081 \cdot 10^{3}$	ρ^9F/T^4	$F24/T^4$
28	$0.3776188652 \cdot 10^{-4}$	$\rho^{11}F/T^2$	$F25/T^2$
29	$-0.3322765123 \cdot 10^{-2}$	$\rho^{11}F/T^3$	$F25/T^3$
30	$0.1791967071 \cdot 10^{-7}$	$\rho^{13}F/T^2$	$F26/T^2$
31	$0.9450766278 \cdot 10^{-5}$	$\rho^{13}F/T^3$	$F26/T^3$
32	$-0.1234009431 \cdot 10^{-2}$	$\rho^{13}F/T^4$	$F26/T^4$

[a] See eqns. 10 and 11.

VISCOSITY

Viscosities were obtained by fitting tabulated viscosity data [5] to the equation

$$\eta_R = \sum_{i=0}^{4} \sum_{j=0}^{4} c_{i,j} T_R^i \rho_R^i \tag{12}$$

The $c_{i,j}$ coefficients for CO_2 are listed in Table II. The fit is applicable for pressures from 40 to 1000 bar over the temperature range 315 to 900 K with an average error of 0.4%.

TABLE II

COEFFICIENTS OF η_R VISCOSITY EQUATION FOR CO_2, $c_{i,j}$[a]

i	j	$c_{i,j}$	i	j	$c_{i,j}$
0	0	1.984239055923858	2	3	−6.962674520424649
0	1	−1.765978814900643	2	4	0.7797272269308236
0	2	1.200587190352171	3	0	−15.836119060967
0	3	−0.3587967344551215	3	1	26.17032056108262
0	4	$3.939799401399628 \cdot 10^{-2}$	3	2	−17.42070707993796
1	0	−6.939097844205919	3	3	5.402335087741039
1	1	12.16864979120884	3	4	−0.6352935554972202
1	2	−7.954279939480736	4	0	4.337989765743405
1	3	2.311176553431279	4	1	−7.058859850635407
1	4	−0.2499449770969321	4	2	4.866472957964851
2	0	22.0798196307882	4	3	−1.607823031693741
2	1	−35.92289143102958	4	4	0.2014049388370968
2	2	23.41530455411397			

[a] See eqn. 12.

For the calculation of reduced viscosity from η/η°, a fit of η° *vs.* T_R was completed, where η° was selected as the viscosity at 1 bar. The relation is

$$\eta^\circ = \sum_{j=0}^{3} a_j T_R^j \tag{13}$$

The a_j coefficients are given in Table III. Figs. 1 and 2 show the relationship of viscosity to pressure and density, respectively.

THE CORE OF THE DISTRIBUTION FUNCTION

In order to obtain a tractable expression for the core of the distribution function for use in the integral equations, the expression $\eta_R^{-1}(\partial P_R/\partial \rho_R)$ was evaluated using the equation of state and tabulated viscosity data [5] and fit to a seventh-order polynomial

TABLE III

COEFFICIENTS OF η° (10^{-6} Ns/m^2) VISCOSITY EQUATION FOR CO_2[a]

j	a_j (10^{-6} Ns/m^2)
0	−1.842303556958221
1	19.94110352045899
2	−3.288620563501078
3	0.3299574285621828

[a] See eqn. 13.

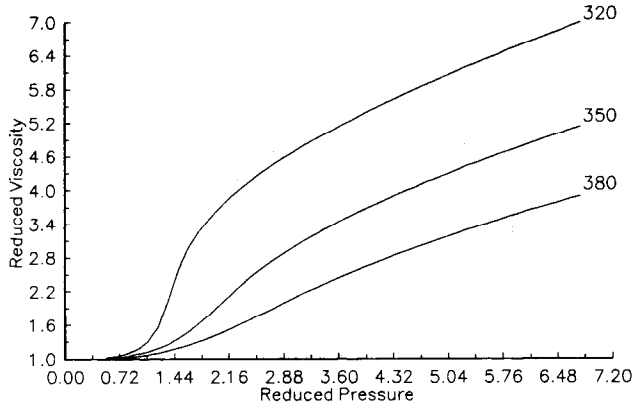

Fig. 1. Relationship between reduced viscosity and reduced pressure of CO_2 at 320, 350 and 380 K.

in reduced density at a given temperature. The resulting equation for the core of the distribution function is

$$\frac{1}{\eta_R}(\partial P_R/\partial \rho_R)_T = \sum_{j=0}^{7} c(T)_j \rho_R^j \tag{14}$$

The coefficients for selected temperatures from 320 to 500 K are given for CO_2 in Table IV. This method has the advantage of yielding analytically solvable integrals for the density averages, but the disadvantage of requiring a temperature-dependent set of coefficients. The equation of state and viscosity equations may be used to calculate these coefficients at any desired temperature. Alternatively, the integrals may be evaluated numerically at any temperature and pressure using the equation of state to obtain $(\partial P_R/\partial \rho_R)_T$ and eqn. 12 to obtain η_R^{-1}.

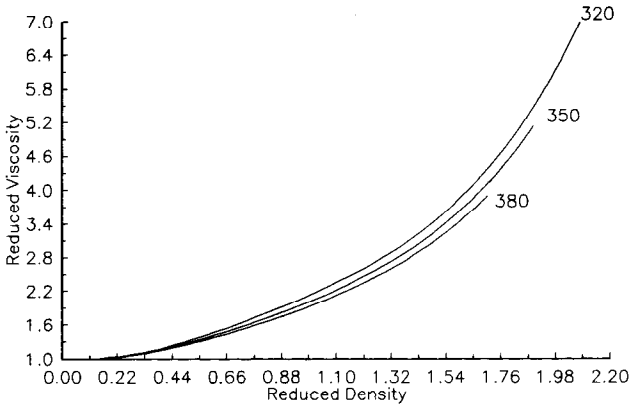

Fig. 2. Relationship between reduced viscosity and reduced density of CO_2 at 320, 350 and 380 K.

TABLE IV

COEFFICIENTS OF THE CORE OF THE DISTRIBUTION FUNCTION, $\eta_R^{-1}(\partial P_R/\partial \rho_R)_T$, FOR CO_2

T/j	0	1	2	3	4	5	6	7
315	3.430721	−5.436177	−14.063478	50.004813	−61.078887	37.082152	−11.123848	1.315836
318	3.449651	−5.165713	−14.619629	50.386233	−61.179006	37.156443	−11.184187	1.329785
320	3.468362	−5.035216	−14.898416	50.693615	−61.520404	37.471557	−11.330728	1.354716
323	3.507241	−4.981013	−14.660994	49.710760	−60.361265	36.903599	−11.220950	1.350461
325	3.529547	−4.900966	−14.704797	49.488739	−60.065716	36.806435	−11.232691	1.357955
328	3.567610	−4.835326	−14.554064	48.740216	−59.183956	36.402942	−11.171629	1.359514
330	3.594037	−4.805044	−14.400660	48.137436	−58.477669	36.057054	−11.105119	1.357108
333	3.634926	−4.775353	−14.113013	47.128036	−57.301045	35.461413	−10.978996	1.349891
335	3.663093	−4.767234	−13.876192	46.368154	−56.417075	34.998493	−10.872244	1.341962
340	3.735941	−4.779590	−13.157321	44.218988	−53.909728	33.635421	−10.531496	1.311594
345	3.811424	−4.829204	−12.292277	41.775228	−51.034637	32.005334	−10.090694	1.266392
350	3.888584	−4.904933	−11.324438	39.117654	−47.871881	30.149953	−9.560026	1.207156
355	3.966580	−4.996535	−10.295859	36.329849	−44.511071	28.120857	−8.954059	1.135399
360	4.044703	−5.094889	−9.245997	33.495104	−41.047809	25.977564	−8.291338	1.053338
365	4.122378	−5.192201	−8.210274	30.692525	−37.578626	23.784241	−7.593386	0.963788
370	4.199161	−5.282081	−7.219233	27.994251	−34.196937	21.606888	−6.883810	0.870070
375	4.274729	−5.359553	−6.297969	25.463207	−30.989408	19.510516	−6.187295	0.775874
380	4.348880	−5.421136	−5.465210	23.149812	−28.030595	17.554815	−5.527916	0.685023
385	4.421507	−5.464634	−4.733836	21.092105	−25.381855	15.792668	−4.928420	0.601345
390	4.492589	−5.489028	−4.111053	19.315239	−23.089491	14.268038	−4.409205	0.528503
395	4.562169	−5.494315	−3.598799	17.831406	−21.183243	13.013900	−3.987211	0.469786
400	4.630341	−5.481284	−3.194661	16.641477	−19.677496	12.052323	−3.675652	0.428020
410	4.762983	−5.406185	−2.684254	15.098625	−17.853463	11.039525	−3.415627	0.403671
420	4.891684	−5.278686	−2.504810	14.525946	−17.471506	11.193787	−3.650242	0.465356
430	5.017609	−5.115442	−2.563619	14.691491	−18.248922	12.347147	−4.339176	0.612149
440	5.141729	−4.931525	−2.769727	15.344966	−19.838448	14.248806	−5.395477	0.833515
450	5.264761	−4.738747	−3.046140	16.257123	−21.891474	16.616550	−6.705176	1.111919
460	5.387171	−4.545277	−3.334909	17.241746	−24.101283	19.178477	−8.146164	1.425930
470	5.509227	−4.356014	−3.597456	18.163942	−26.227172	21.702104	−9.603891	1.753273
480	5.631051	−4.173312	−3.811609	18.937261	−28.100147	24.008383	−10.981440	2.073214
490	5.752686	−3.997791	−3.967820	19.516300	−29.618699	25.975777	−12.205201	2.368296
500	5.874126	−3.829018	−4.064945	19.885808	−30.735909	27.534386	−13.225300	2.625066
510	5.995350	−3.666042	−4.107097	20.051584	−31.446624	28.657725	−14.014026	2.834337
520	6.116340	−3.507723	−4.101016	20.032035	−31.774063	29.352199	−14.562299	2.990911
530	6.237089	−3.352985	−4.054338	19.851937	−31.758491	29.646665	−14.875213	3.092957
540	6.357602	−3.200899	−3.974493	19.538255	−31.449228	29.584628	−14.968485	3.141461
550	6.477901	−3.050744	−3.868163	19.117157	−30.897801	29.216445	−14.864230	3.139390
560	6.598021	−2.902022	−3.740895	18.612604	−30.154598	28.595194	−14.588566	3.091189
570	6.718008	−2.754413	−3.597292	18.045621	−29.266003	27.772556	−14.168946	3.002157
580	6.837917	−2.607786	−3.440735	17.433791	−28.273103	26.796665	−13.632527	2.877999
590	6.957805	−2.462108	−3.273899	16.791695	−27.211291	25.710798	−13.005036	2.724506
600	7.077740	−2.317489	−3.098509	16.130949	−26.110274	24.552744	−12.309946	2.547261

The core of the distribution function is shown as a function of pressure and density in Figs. 3 and 4, respectively.

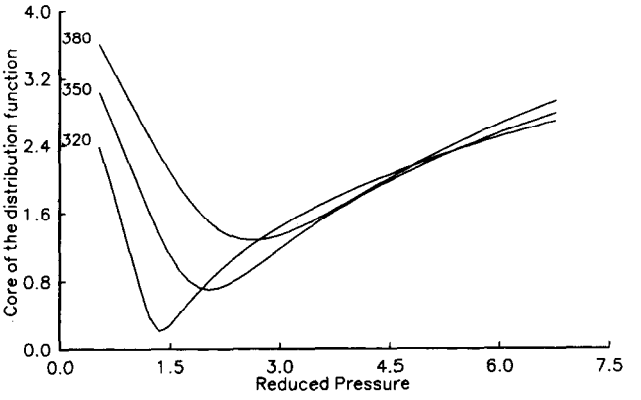

Fig. 3. Relationship between the "core" of the distribution function and reduced pressure for CO_2 at 320, 350 and 380 K.

COLUMN AVERAGES

Typical inlet and outlet pressures were selected and the corresponding densities calculated from the equation of state. The positional and temporal average densities were calculated using the seventh-order polynomial for the core of the distribution function (eqn. 14):

The mean density

$$\overline{\rho_R} = \frac{\rho_{R,i} + \rho_{R,o}}{2} \tag{15}$$

The spatial average density

$$<\rho_R>_x = \sum_{j=3}^{10} c_{j-3}(\rho_{R,i}^j - \rho_{R,o}^j)/j \Big/ \sum_{j=2}^{9} c_{j-2}(\rho_{R,i}^j - \rho_{R,o}^j)/j \tag{16}$$

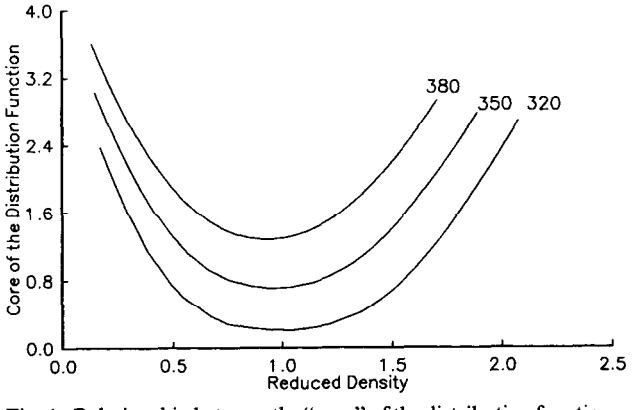

Fig. 4. Relationship between the "core" of the distribution function and reduced density for CO_2 at 320, 350 and 380 K.

The temporal average density

$$<\rho_R>_t = \sum_{j=4}^{11} c_{j-4}(\rho^j_{R,i} - \rho^j_{R,0})/j \Big/ \sum_{j=3}^{10} c_{j-3}(\rho^j_{R,i} - \rho^j_{R,0})/j \qquad (17)$$

Table V summarizes the results for selected outlet and inlet pressures at 320 K. Note that for a pressure drop of 50 bar, there is a significant difference between the positional and temporal average densities for low outlet densities, but they are essentially equal if the outlet density is high.

COLUMN AVERAGE (OBSERVED) CAPACITY FACTOR

The observed or apparent capacity factor was calculated assuming the form $k'_{local} = k'_0 \exp(a\rho + b\rho^2)$ for the local capacity factor, where k'_0 refers to the zero-density value. The constants for this expression were calculated for heptadecane and octadecane from ref. 6:

$$\ln k'_0 = -(4.43 + 0.784n) + [(1.09 + 1.676n)/T_R]$$

$$a = (0.40 + 0.595n) - (0.97 + 1.448n)/T_R$$

$$b = (0.17 + 0.260n)/T_R \qquad (18)$$

TABLE V

AVERAGE DENSITIES AT 320 K

P_i (bar)	$\rho_{R,i}$	P_0 (bar)	$\rho_{R,0}$	$\overline{\rho_R}^a$	$<\rho_R>_x^b$	$<\rho_R>_t^c$
80	0.49	70	0.38	0.44	0.44	0.44
90	0.67	70	0.38	0.53	0.51	0.53
100	0.96	70	0.38	0.67	0.62	0.67
110	1.21	70	0.38	0.80	0.76	0.85
120	1.35	70	0.38	0.87	0.88	0.99
130	1.44	70	0.38	0.91	0.97	1.09
110	1.21	100	0.96	1.08	1.10	1.10
120	1.35	100	0.96	1.16	1.19	1.20
130	1.44	100	0.96	1.20	1.26	1.28
140	1.51	100	0.96	1.23	1.31	1.33
150	1.56	100	0.96	1.26	1.35	1.37
160	1.60	100	0.96	1.28	1.39	1.41
140	1.51	130	1.44	1.48	1.48	1.48
150	1.56	130	1.44	1.50	1.50	1.51
160	1.60	130	1.44	1.52	1.53	1.53
170	1.63	130	1.44	1.54	1.55	1.55
180	1.66	130	1.44	1.55	1.57	1.57
190	1.69	130	1.44	1.57	1.59	1.59

[a] See eqn. 15.
[b] See eqn. 16.
[c] See eqn. 17.

where n = number of carbon atoms in the alkane. The numerator in eqn. 5 was evaluated numerically using a numerical integration routine [7].

The separation factor, α, for heptadecane and octadecane was calculated from

$$\alpha = \frac{<k'>_{t,C_{18}}}{<k'>_{t,C_{17}}} \tag{19}$$

The approximation

$$<k'>_t \approx k_0 \exp(a<\rho_R>_t + b<\rho_R^2>_t)$$

or

$$\ln <k'>_t \approx \ln k_0 + a<\rho_R>_t + b<\rho_R^2>_t \tag{20}$$

was tested. As expected [1], the estimated value is always less than or equal to the value for $\ln <k'>_t$ calculated from eqn. 5, and is essentially equal to the calculated value if the outlet density is close to the inlet density (as in capillary SFC) or if the outlet density is significantly greater than the critical density (Fig. 5). The estimated α values are also close to the calculated values under these conditions. In general, low densities produce higher α values. For a given outlet pressure, low density drops also produce higher α values. Although high densities and/or high density drops lead to shorter analysis times, large density drops are undesirable because they may lead to greater band broadening [8]. As long as the chromatographic conditions are in the region where the estimates are close to the calculated values, both $\ln <k'>$ and α can be easily estimated for a given set of conditions if the local capacity factors are known. The temporal average density can be replaced by the arithmetic mean density, thus simplifying the calculation. However, the column average density is significantly different from the inlet density, so the capacity factor cannot be approximated using the inlet density alone. The results are summarized in Table VI where column 1 is the temporal average density from Table V.

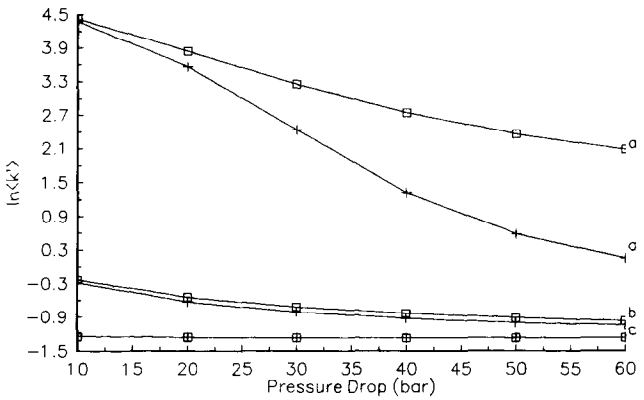

Fig. 5. Average capacity factor as a function of pressure drop. (□) Calculated from eqn. 5; (+) estimated from eqn. 20. (a) P_0 = 70 bar; (b) P_0 = 100 bar; (c) P_0 = 130 bar.

TABLE VI

CALCULATED AND ESTIMATED ln $<k'>$ VALUES

$<\rho_R>_t$	ln $<k'>$ Num.[a] C_{17}	ln $<k'>$ Est.[b] C_{17}	ln $<k'>$ Num.[a] C_{18}	ln $<k'>$ Est.[b] C_{18}	α Num.[c]	α Est.[d]
P_0 = 70 bar ($\rho_{R,0}$ = 0.38)						
0.44	4.42	4.37	4.89	4.83	1.61	1.60
0.53	3.84	3.56	4.29	3.98	1.57	1.53
0.67	3.25	2.44	3.69	2.80	1.56	1.43
0.85	2.74	1.32	3.18	1.62	1.55	1.34
0.99	2.36	0.59	2.80	0.85	1.55	1.29
1.09	2.08	0.15	2.51	0.38	1.54	1.26
P_0 = 100 bar ($\rho_{R,0}$ = 0.96)						
1.10	−0.23	−0.28	−0.02	−0.07	1.24	1.23
1.20	−0.55	−0.63	−0.35	−0.44	1.22	1.20
1.28	−0.72	−0.82	−0.54	−0.64	1.21	1.19
1.33	−0.84	−0.93	−0.66	−0.76	1.20	1.19
1.37	−0.92	−1.01	−0.74	−0.84	1.19	1.18
1.41	−0.97	−1.06	−0.80	−0.89	1.19	1.18
P_0 = 130 bar ($\rho_{R,0}$ = 1.44)						
1.48	−1.25	−1.25	−1.09	−1.09	1.16	1.16
1.51	−1.26	−1.26	−1.11	−1.11	1.16	1.16
1.53	−1.27	−1.27	−1.12	−1.12	1.16	1.16
1.55	−1.28	−1.28	−1.12	−1.12	1.16	1.16
1.57	−1.27	−1.27	−1.12	−1.12	1.16	1.16
1.59	−1.27	−1.27	−1.12	−1.12	1.16	1.16

[a] Numerical integration of eqn. 5.
[b] Estimated from eqn. 20.
[c] Determined from numerically integrated values of ln $<k'>$.
[d] Determined from estimated values of ln $<k'>$.

COLUMN PROFILES

The density decrease over the column was divided into ten equally spaced density decrements from the inlet to the outlet density. Profiles for the mobile phase were generated using eqns. 6 and 7 and the core of the distribution function:

$$x/L = \sum_{j=2}^{9} c_{j-2}(\rho_{R,i}^{j} - \rho_{R}^{j})/j \Big/ \sum_{j=2}^{9} c_{j-2}(\rho_{R,i}^{j} - \rho_{R,0}^{j})/j \tag{21}$$

$$\frac{\tau_u}{t_u} = \sum_{j=3}^{10} c_{j-3}(\rho_{R,i}^{j} - \rho_{R}^{j})/j \Big/ \sum_{j=3}^{10} c_{j-3}(\rho_{R,i}^{j} - \rho_{R,0}^{j})/j \tag{22}$$

The fractional solute migration time was calculated by numerical integration of eqn. 8. The results are summarized in Table VII. Note that when the mobile phase has spent 50% of its time on the column, it has traversed 47% of the column length. At this point, the reduced density is 1.11, compared to 1.09, the arithmetic mean density. Hence, the mobile phase spends *relatively* more time in the inlet region of the column. The solutes

TABLE VII

COLUMN PROFILES

T = 320 K, P_0 = 100 bar, P_i = 110 bar.

ρ_R	x/L[a]	τ_u/t_u[b]	τ_s/t_s[c] C_{17}	τ_s/t_s[c] C_{18}	α[d]
1.21	0.00	0.00	0.00	0.00	–
1.19	0.13	0.14	0.12	0.12	1.20
1.16	0.25	0.27	0.24	0.23	1.21
1.14	0.37	0.39	0.34	0.33	1.21
1.11	0.47	0.50	0.44	0.43	1.21
1.09	0.57	0.60	0.54	0.53	1.21
1.06	0.66	0.69	0.63	0.62	1.22
1.04	0.75	0.78	0.72	0.71	1.22
1.01	0.84	0.85	0.82	0.81	1.23
0.99	0.92	0.93	0.91	0.90	1.23
0.96	1.00	1.00	1.00	1.00	1.24

[a] See eqn. 21.
[b] See eqn. 22.
[c] See eqn. 8.
[d] See eqn. 19.

are moving relatively more quickly because they have a much smaller k' in the higher-density inlet part. The effective separation factor, α, which is defined as the ratio of temporal average capacity factors of the two solutes at a given value of x/L, increases as the column is traversed. This does not necessarily imply, however, that longer columns will produce better separations. The change in α is a pressure-drop-induced effect; the same pressure drop can also cause increased band spreading [8]. Indeed, it is conceivable that shorter columns could provide separations with resolution equal or superior to that from longer columns.

CONCLUSIONS

If the pressure drop over a column is small, or if the outlet density is sufficiently greater than the critical density, the arithmetic mean density, the positional average density and the temporal average density are nearly identical. The average capacity factor can then be related to the local capacity factor and the average density using any of the density averages and eqn. 20. However, if the density drop is large and encompasses the region where the core of the distribution function goes through a minimum (Fig. 4), the average capacity factor must be calculated using eqn. 5 and a numerical integration routine. It is then difficult to relate the observed capacity factor to the local capacity factor. This problem is still under investigation. It is also possible that Darcy's law may not be applicable when pressure drops are high since high mobile-phase velocities may lead to turbulence. A simpler expression for the core of the distribution function would lead to more tractable expressions for both the density averages and the apparent capacity factor.

ACKNOWLEDGEMENTS

This material is based upon work supported at Georgetown University by the National Science Foundation under Grant CHE-8902735, which the authors gratefully acknowledge. The Bush Sabbatical Program of the University of Minnesota is also thanked for partial support of D.P. T.B. acknowledges support of the Gas Research Institute and the U.S. Department of Energy.

REFERENCES

1 D. E. Martire, *J. Chromatogr.*, 461 (1989) 165.
2 R. T. Jacobsen and R. J. Stewart, *J. Phys. Chem. Ref. Data*, 2 (1973) 757.
3 J. F. Ely, *Proceedings of the 63rd Gas Processors Association Annual Convention*, Gas Processors Association, Tulsa, OK, 1984, pp. 9–22.
4 G. Arfken, *Mathematical Methods for Physicists*, Academic Press, Orlando, FL, 3rd ed., 1985, p. 964.
5 K. Stephan and K. Lucas, *Viscosity of Dense Fluids*, Plenum Press, New York and London, 1979.
6 D. E. Martire and R. E. Boehm, *J. Phys. Chem.*, 91 (1987) 2433.
7 T. E. Sharp, *Applied Numerical Methods for the Microcomputer*, Prentice-Hall, Englewood Cliffs, NJ, 1984.
8 D. P. Poe and D. E. Martire, *J. Chromatogr.*, 517 (1990) 3.